



Synthesis and characterization of nanostructured palladium-perovskites: Evaluation of their catalytic activity in cross-coupling chemistry

A. Essoumhi^{1*}, A. Solhy², S. El Kazzouli^{3*}

¹Faculté Polydisciplinaire, Université Sultan Moulay Slimane, 23000, Béni-Mellal, Morocco

²Université Mohammed VI Polytechnique, Ben Guerir, Morocco

³Euromed Research Institute, Euro-Mediterranean University of Fes (UEMF), Fès-Shore, Route de Sidi Hrazem, 30070, Fès, Morocco

Received 15 Dec 2015, Revised 31 Jan 2016, Accepted 12 Feb 2016

*Corresponding author: E-mail: a.essoumhi@gmail.com ; Tel: (+212611981657) and s.elkazzouli@ueuromed.org; Tel: (+212661299565)

Abstract

LaFe_{0.57}Co_{0.38}Pd_{0.05}O₃ perovskite-type oxide catalysts were synthesized via flash combustion method. Then, their structural and textural properties were studied. Depending on the thermal treatment, amorphous or crystalline materials with different particle sizes were obtained. The catalytic activity of these systems was investigated in Suzuki-Miyaura and Sonogashira cross-coupling reactions. Mechanistic studies demonstrated that the materials operate following “release and catch” mechanism. “Ingress and Egress” of palladium in perovskite systems constitute a driving force for the preparation of new chemicals with low metal contamination.

Keywords: perovskite, palladium, cross-coupling, Suzuki-Miyaura, Sonogashira, heterogeneous catalysis

Introduction

The homogeneous catalysis suffers from numerous drawbacks, mainly, high cost, non-reusability of catalyst, as well as the environmental pollution caused by the use of organic solvents and the heavy metallic ions. In addition, the homogeneous palladium-catalyzed coupling reactions lead to final products but with high impurities of residual metals which limit their application, particularly, in pharmaceutical fields [1-7]. In addition, high cost of palladium makes its recovery and reuse highly desirable. Hence, good heterogeneous candidates have to be assessed in terms of their activity and selectivity, metal leaching resistance and considering catalyst lifetime and reusability [8]. The development of heterogeneous Pd catalytic systems seems a promising option to address these problems. However, the heterogeneous Pd catalyst activity, selectivity, leaching resistance, lifetime (stability), and reusability have to be improved. Up to now, many solid systems containing Pd nanoparticles have proved to be good catalysts for the carbon-carbon bond forming reactions in very heterogeneous media [9-12].

Perovskite based materials are exciting carriers to host palladium catalysts with an enhanced tolerance factor of 0.9 (Goldschmidt factor) [13]. They are also able to stand harsh basic conditions often necessary for the achievement of cross-coupling reactions such as Suzuki-Miyaura and Sonogashira. This specificity makes perovskite based materials valuable candidates to substitute the Pd catalyst supported on charcoal (Pd/C) or on silica based materials (Pd/SiO₂) [14].

Various supports containing Pd have been developed including activated carbon [15-17], zeolites and molecular sieves [18-20] metal oxides [21-23], clays [24, 25] earth salts, porous glass [26, 27] and organic polymers [28]. The advantage of Pd-containing perovskite systems is that Pd can be reversibly incorporated into the lattice on oxidation and segregated out as small particles. A few studies reported the self-regeneration of the catalyst [13, 29-31].

Activity and stability of the catalysts are strongly related to material properties such as particle size and particle size distribution, morphology and crystallinity that are on their turn controlled by the methods used for their preparation [32].

2. Materials and methods

2.1. Apparatus

LaFe_{0.57}Co_{0.38}Pd_{0.05}O₃ powder was synthesized via flash combustion method. Starting materials were analytical grade La(NO₃)₃·6H₂O, Fe(NO₃)₃·9H₂O, Co(NO₃)₂·6H₂O, Pd(NO₃)₂·2H₂O and glycine. The nitrates serve as oxidants while the glycine serves both as fuel and as chelating agent for metal ions. The appropriate molar ratios of nitrates and glycine were mixed in a minimum amount of deionized water to obtain a limpid solution. A glycine to nitrate ratio of 1:2.5 was used. The aqueous solution was concentrated on a hot plate at 200°C, generating a viscous liquid. Upon complete evaporation of the water, the dried mixture was placed into an oven at 400°C to start the combustion reaction which occurred within 2-3 min. The optimum conditions for calcination were determined by TGA (Q50) between room temperature and 900 °C, and the heating rate was 10 °C min⁻¹. The powder obtained was annealed at 600°C and 800°C for 1h. The morphology and the grain size after annealing at 600°C and 800°C were observed by transmission electron microscopy (TEM, FEI Tecnai) and scanning electron microscopy (SEM, FEI Quanta 200). X-ray diffraction (XRD) data were obtained by D8 Advance Bruker with CuK α radiation operated at 45 kV and 100 mA. The diffractometer data were recorded for 2 θ values between 10° and 90°. JCPDS powder diffraction database was used for phase analysis.

3. Results and discussion

3.1. Thermal decompositions and structural properties

The thermal decomposition of the complex precursor was investigated by TG, as shown in Fig. 1. The TG curve of the complex pyrolysis exhibits characteristically a three-stage weight loss profile. The first stage of the TG profile is reached at 30–120 °C, which is attributed to the loss of water physisorbed. The second stage is a sharp weight loss of about 30% between 200 and 700 °C, which is due to the oxidative decomposition of the organic complexing species and departure of nitrate. The third stage is a gradual weight loss between 700 and 800 °C, which is due to the thermal decomposition of carbonates and the formation of perovskite structure.

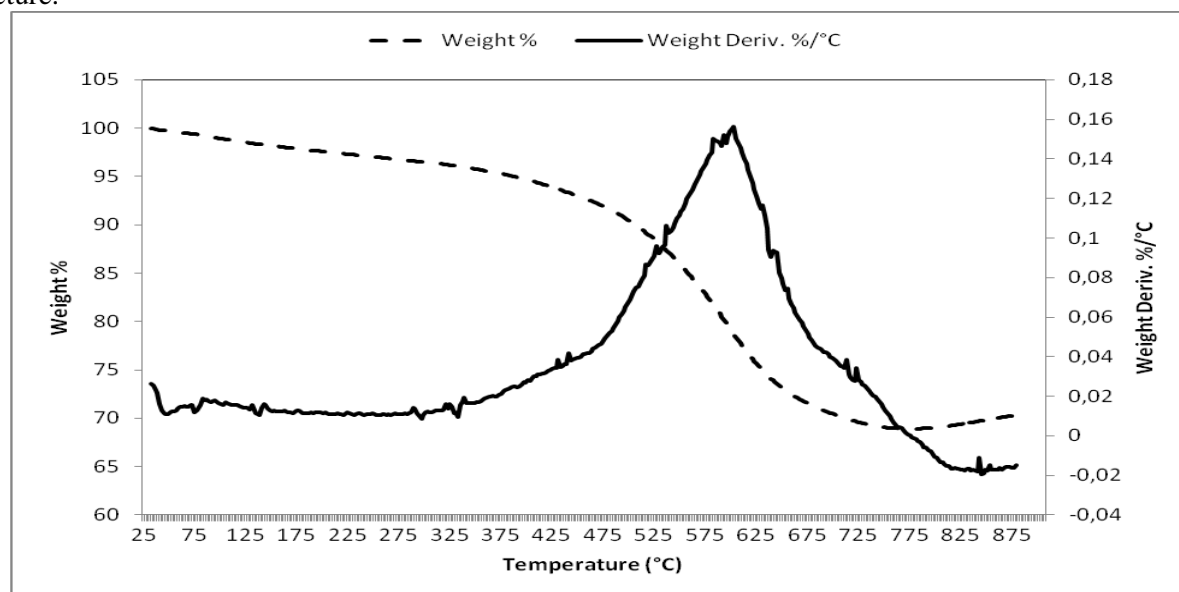


Figure 1: TGA thermogram of LaFe_{0.57}Co_{0.38}Pd_{0.05}O₃.

X-ray diffraction was performed on LaFe_{0.57}Co_{0.38}Pd_{0.05}O₃ after annealing at 400°C, 600°C and 800°C for 1h in order to check the purity of the crystalline product and to allow estimation of the crystallite size of the powder. The annealing at 400 °C shows that the product is still amorphous. A calcination at 600°C and 800 °C leads to a dominant perovskite with orthorhombic phase structure, space group Pnma (reference pattern 44-0361). Particle sizes of as-synthesized and calcined Perovskite powders were estimated by using full width at half maxima (FWHM) of the major (112) XRD peak with the Scherrer's formula assuming spherical particles, $D = 0.9\lambda/\beta\cos\theta$ where D is the particle size, λ is the X-ray radiation wavelength, θ is the angle of XRD peak, and β (in radians) is the FWHM of the XRD peak. θ and β were determined by using the Topas software

(Bruker) with the Gaussian profile to fit the XRD peak. It was found that the particle size of powders calcined at 600 and 800 °C are respectively, 25 nm and 36 nm.

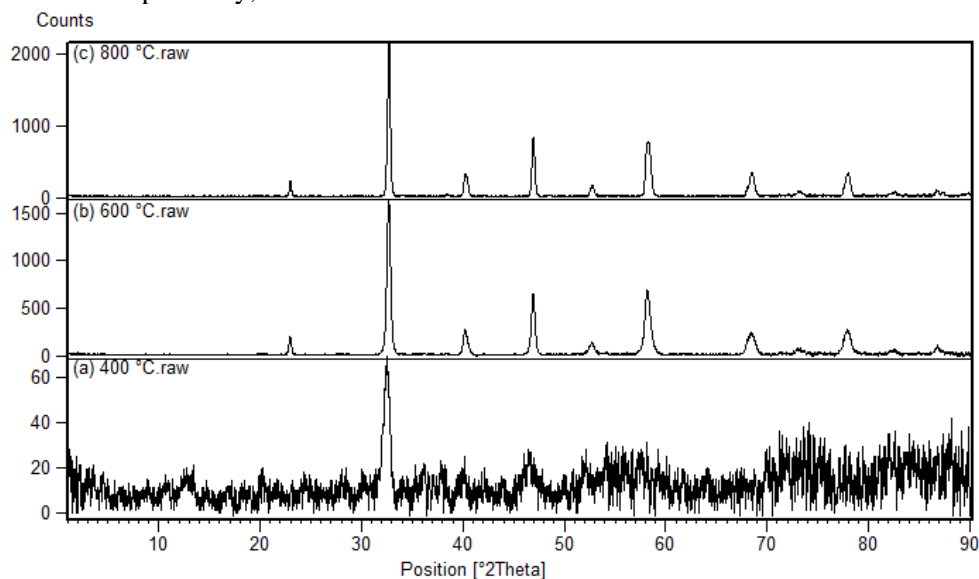


Figure 2: X-ray diffraction patterns of $\text{LaFe}_{0.57}\text{Co}_{0.38}\text{Pd}_{0.05}\text{O}_3$ powder annealed at a) 400 °C, b) 600 °C and c) 800 °C.

3.2 TEM and SEM

Size and morphology of different perovskite powders were observed by TEM and SEM. Fig. 3 shows that the perovskite is composed of crystallites strongly linked by grain boundaries or material bridges, creating inter-granular porosity. The particle size for powder annealed at 600 °C and 800 °C were respectively estimated about 50 and 100 nm. The difference of these sizes compared to the crystallite size measured from the X-ray diffraction using Debye Scherrer formula, shows that we have aggregates resulting from the melting of the particles as observed on TEM images.

Surface area from nitrogen sorption analysis for powder annealed at 400, 600 and 800 °C are respectively about 25, 16 and 8 m^2/g . The isotherm profile, from nitrogen sorption analysis, indicates that the accessible porous network is related to the inter-particle void volume. The crystallization induces sintering of the crystals and decreases the specific surface area. These results are consistent with those previously published, for example Sina et al. found for LaCoO_3 and $\text{LaCo}_{0.95}\text{Pd}_{0.05}\text{O}_3$ calcined at 700°C 4.9 and 6.9 m^2/g , respectively [33], while Kaliaguine et al. published for LaFeO_3 , $\text{LaFe}_{0.8}\text{Cu}_{0.2}\text{O}_3$ and $\text{LaFe}_{0.97}\text{Pd}_{0.03}\text{O}_3$ calcined at 500 °C the slightly good specific surface area respectively 30, 41 and 48 m^2/g [34]. Despite good catalytic activity, the increase in surface area is still a major challenge for this type of material.

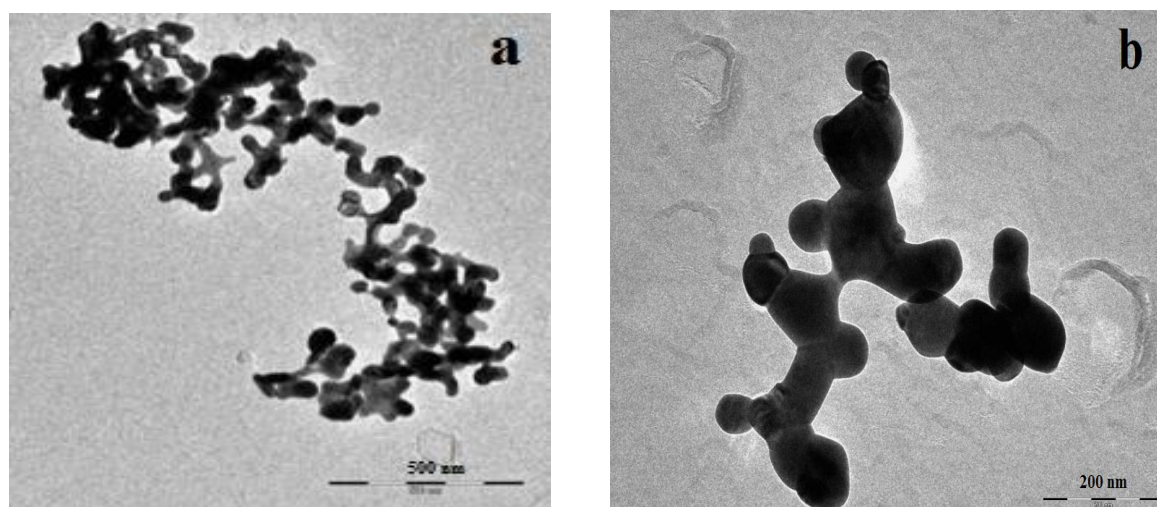


Figure 3: TEM image of powder annealed at a) 600 °C and b) 800 °C.

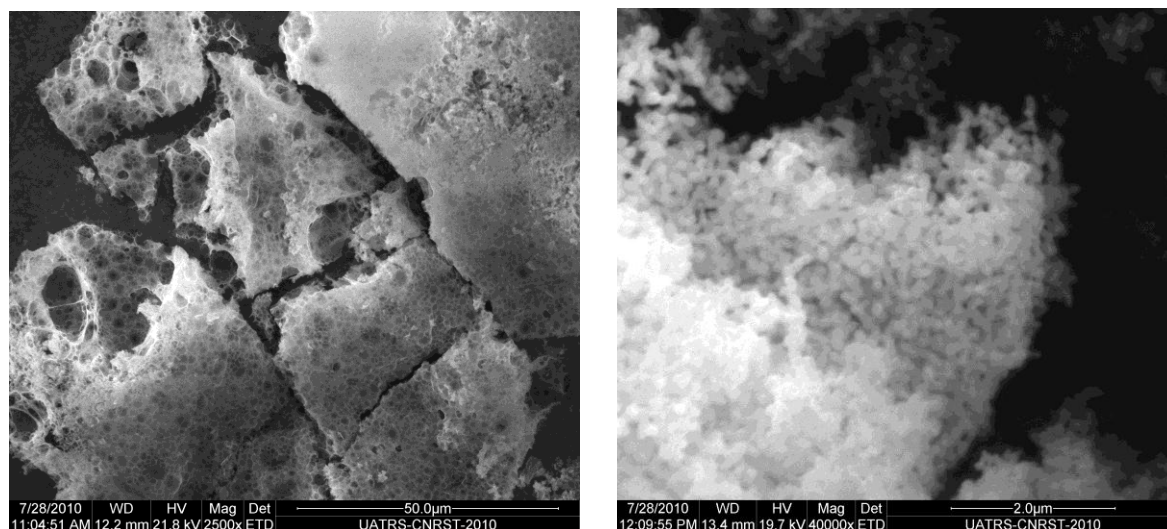


Figure 4: SEM image of powder annealed at a) 400 °C and b) 800 °C.

3.2 Catalytic activity

To evaluate the catalytic activity of $\text{LaFe}_{0.57}\text{Co}_{0.38}\text{Pd}_{0.05}\text{O}_3$ annealed at three different temperatures (400 °C (catalyst A), 600 °C (catalyst B) and 800 °C (catalyst C)), we selected two important cross-coupling reactions (Suzuki-Miyaura and Sonogashira). After various optimizations of the reactions under standard conditions for both Suzuki-Miyaura [35, 36] and Sonogashira [37, 38] in the presence of either catalyst A, B or C, we observed for both cross-coupling reactions (Suzuki-Miyaura and Sonogashira) that catalyst A gave very low reaction yields. However, when catalysts B and C were used, total reaction conversions were achieved. Catalyst B was selected because it is easier to prepare and it achieved cross-coupling with better reaction times compared to catalyst C: (30 min (with catalyst B) instead of 45 min (catalyst C) for Suzuki-Miyaura coupling and 40 min under Millstone microwave (MW) (catalyst B) instead of 60 min under MW (catalyst C)). This difference in the reaction times can be explained by the specific surface area of catalyst B ($16 \text{ m}^2/\text{g}$) which is two fold higher than catalyst C ($8 \text{ m}^2/\text{g}$).

In the case of Suzuki-Miyaura cross-coupling, the reaction was carried out using the following conditions (1.2 equivalents of 4-methoxyphenyl boronic acid, 2 equivalents of K_2CO_3 , H_2O , MW, 140 °C, 30 min) [35] which led to the desired compound 1 in 90% yield (Scheme 1).

Scheme 1: Suzuki-Miyaura and Sonogashira cross-coupling reactions.

Sonogashira cross-coupling reaction was investigated under both microwave and conventional heating conditions using the following conditions (2.5 mol% of $\text{LaFe}_{0.57}\text{Co}_{0.38}\text{Pd}_{0.05}\text{O}_3$ in the presence of 2 equivalents

of Na₂CO₃ (dissolved in water), 1 equivalent of BTBA (tetra *n*-butylammonium bromide, 1 equivalent of 3-bromotoluene, 2.2 equivalents of phenylacetylene in DMF as solvent at 150°C [37]. A total conversion was obtained after 40 min under microwave irradiation while, in refluxing DMF, 20 hours of the reaction times was needed to achieve a total conversion. The expected compound 2 was isolated in 92% yield (under microwave) and with a slightly lower yield under conventional heating (89%) (Scheme 1). The structures of compounds 1 and 2 were confirmed by ¹H NMR, ¹³C NMR, melting point and mass spectroscopy analyses. These data are comparable to those reported in the literature [39, 40].

Conclusion

In this work, LaFe_{0.57}Co_{0.38}Pd_{0.05}O₃ was synthesized by flash combustion method which is a simple and easy way for the preparation of the catalyst nanoparticles with sizes ranging between 50 and 100 nm. The catalytic activity of LaFe_{0.57}Co_{0.38}Pd_{0.05}O₃ annealed at 600 °C was investigated toward Suzuki-Miyaura and Sonogashira cross-coupling reactions leading to the desired products in excellent yields. The investigation of LaFe_{0.57}Co_{0.38}Pd_{0.05}O₃ catalyst in other key cross-coupling reactions is undergoing.

Acknowledgments-The authors wish to thank Professors El Kadib and El Brahmī for their help.

References

1. Magano J., Dunetz J. R., *Chem. Rev.* 111 (2011) 2177.
2. Beletskaya I. P., Ananikov V. P., *Chem. Rev.* 111 (2011) 1596.
3. Selander N., Szabo K. J., *Chem. Rev.* 111 (2011) 2048.
4. Mkhali I. A. I., Barnard J. H., Marder T. B., Murphy J. M., Hartwig J. F., *Chem. Rev.* 110 (2010) 890.
5. Yin L., Liebscher J., *Chem. Rev.* 107 (2007) 133.
6. Garrett C. E. Prasad K., *Adv. Synth. Catal.* 346 (2004) 889.
7. Konisberger K., Chen G. P., Wu R. R., Girgis M. J., Prasad K., Repic O., Blacklock T., *J. Org. Process Res. Dev.* 7 (2003) 733.
8. Molnar A., *Chem. Rev.* 111 (2011) 2251.
9. Son S.U., Jang Y., Park J., Na H.B., Park H.M., Yun H.J., Lee J., Hyeon T., *J. Am. Chem. Soc.* 126 (2004) 5026.
10. Consorti C.S., Flores F.R., Dupont J., *J. Am. Chem. Soc.* 127 (2005) 12054.
11. Sawai K., Tatumi R., Nakahodo T., Fujihara H., *Angew. Chem. Int. Ed.* 47 (2008) 6917.
12. Lia H., Zhua Z., Lia H., Lib P., Zhou X., *J. Colloid Interface Sci.* 349 (2010) 613.
13. Nishihata Y., Mizuki J., Akao T., Tanaka H., Uenishi M., Kimura M., Okamoto T., Hamada N., *Nature*, 418 (2002) 164.
14. Yin L., Liebscher J. *Chem. Rev.* 107 (2007) 133.
15. Seki M. *Synthesis*, 18 (2006) 2975.
16. Hagiwara H., Shimizu Y., Hoshi T., Suzuki T., Ando M., Ohkubo K., Yokoyama C., *Tetrahedron Lett.* 42 (2001) 4349.
17. Zhao F., Shirai M., Arai M., *J. Mol. Catal. A: Chem.* 154 (2000) 39.
18. Toebes M. L., van Dillen J. A., de Jong K. P., *J. Mol. Catal. A: Chem.* 173 (2001) 75.
19. Mehnert C.P., Weaver D.W., Ying J.Y., *J. Am. Chem. Soc.* 120 (1998) 12289.
20. Djakovitch L., Koehler K., *J. Am. Chem. Soc.* 123, (2001) 5990.
21. Biffis A., Zecca M., Basato M., *Eur. J. Inorg. Chem.* 5 (2001) 1131.
22. Wagner M., Köhler K., Djakovitch L., Weinkauff S., Hagen V., Muhler M., *Top. Catal.* 13 (2000) 319.
23. Köhler K., Wagner M., Djakovitch L. *Catal. Today*, 66 (2001) 105.
24. Ramchandani R.K., Uphade B.S., Vinod M.P., Wakharkar R.D., Choudhary V.R., Sudalai A. *Chem. Commun.* 21 (1997) 2071.
25. Varma R.S., Naicker K.P., Liesen P.J., *Tetrahedron Lett.* 40, 2075 (1999).
26. Li J., Mau A.W.H., Strauss C.R., *Chem. Commun.* 14 (1997) 1275.

27. Solodenko W., Wen H., Leue S., Stuhlmann F., Sourkouni-Argirusi G., Jas G., Schönfeld H., Kunz U., Kirschning A., *Eur. J. Org. Chem.*, 17 (2004) 3601.
28. Biffis A., Zecca M., Basato M., *J. Mol. Catal. A: Chem.*, 173 (2001) 249.
29. Nishihata Y., Mizuki J., Tanaka H., Uenishi M., Kimura M., *J. Phys. Chem. Solids*, 66 (2005) 274.
30. Tanaka H., Uenishi M., Taniguchi M., Tan I., Narita K., Kimura M., Kaneko K., Nishihata Y., Mizuki J., *Catal. Today*, 117 (2006) 321.
31. Uenishia M., Taniguchi M., Tanaka H., Kimura M., Nishihata Y., Mizuki J., Kobayashie T., *Appl. Catal. B-Environ.* 57 (2005) 267.
32. Essoumhi A., El Kazzouli S., Bousmina M., *J. Nanosci. Nanotechnol.* 14 (2014) 2012.
33. Sartipi S., Khodadadi A. A., Mortazavi Y., *Appl. Catal. B-Environ.* 83 (2008) 214.
34. Zhang R., Villanueva A., Alamdari H., Kaliaguine S., *J. Catal.* 237 (2006) 368.
35. Kazmaier U., Hähn S., Weiss T. D., Kautenburger R., Maier W. F., *Synlett* 16 (2007) 2579.
36. a) Ben-Yahia A., Naas M., El Brahmī N., El Kazzouli S., Majoral J.-P., Essassi E.M., Guillaumet G., *Curr. Org. Chem.* 17 (2012) 304. b) Koubachi J., El Kazzouli S., Berteina-Raboin S., Mouaddib A., Guillaumet G., *J. Org. Chem.* 72 (2007) 7650.
37. Lohmann S., Andrews S. P., Burk B. J., Smith M. D., Attfield J. P., Tanaka H., Kaneko K., Ley S. V., *Synlett* 8 (2005) 1291.
38. El Kazzouli S., Bouissane L., Khouili M., Guillaumet G., *Tetrahedron Lett.* 46 (2005) 6163.
39. Rao M. L.N., Jadhav D. N., Banerjee D., *Tetrahedron*, 64 (2008) 5762. b) Bhunia, S., Abu Sohel, S. M., Yang, C-C., Lush S-F., Shen F-M., Liu R-S., *J. Organomet. Chem.* 694 (2009) 566.
40. Suzuka T., Okada Y., Ooshiro K., Uozumi Y., *Tetrahedron*, 66 (2008) 10649.

(2016) ; <http://www.jmaterenvirosci.com/>